LETTERS

Ferroelectricity from iron valence ordering in the charge-frustrated system $LuFe_2O_4$

Naoshi Ikeda[1], Hiroyuki Ohsumi[1], Kenji Ohwada[2], Kenji Ishii[2], Toshiya Inami[2], Kazuhisa Kakurai[3], Youichi Murakami[4], Kenji Yoshii[2], Shigeo Mori[5], Yoichi Horibe[5] & Hijiri Kitô[6]

Ferroelectric materials are widely used in modern electric devices such as memory elements, filtering devices and high-performance insulators. Ferroelectric crystals have a spontaneous electric polarization arising from the coherent arrangement of electric dipoles[1] (specifically, a polar displacement of anions and cations). First-principles calculations[2,3] and electron density analysis[4] of ferroelectric materials have revealed that the covalent bond between the anions and cations, or the orbital hybridization of electrons on both ions, plays a key role in establishing the dipolar arrangement. However, an alternative model—electronic ferroelectricity[5]—has been proposed in which the electric dipole depends on electron correlations, rather than the covalency. This would offer the attractive possibility of ferroelectric materials that could be controlled by the charge, spin and orbital degrees of freedom of the electron. Here we report experimental evidence for ferroelectricity arising from electron correlations in the triangular mixed valence oxide, $LuFe_2O_4$. Using resonant X-ray scattering measurements, we determine the ordering of the Fe^{2+} and Fe^{3+} ions. They form a superstructure that supports an electric polarization consisting of distributed electrons of polar symmetry. The polar ordering arises from the repulsive property of electrons—electron correlations—acting on a frustrated geometry.

Mixed valence material $LuFe_2O_4$ is a member of the RFe_2O_4 family, where R are rare-earth elements from Dy to Lu and Y (ref. 6). The crystal structure consists of the alternate stacking of triangular lattices of rare-earth elements, iron and oxygen. An equal amount of Fe^{2+} and Fe^{3+} coexists at the same site in the triangular lattice. Compared with the average iron valence of $Fe^{2.5+}$, Fe^{2+} and Fe^{3+} are considered as having an excess and a deficiency of half an electron, respectively. The coulombic preference for pairing of 'oppositely' signed charges (Fe^{2+} and Fe^{3+}) is considered to cause the degeneracy in the lowest energy for the charge configuration in the triangular lattice, similarly to the triangular antiferromagnetic Ising spins. Thus, RFe_2O_4 is considered to be a charge-frustrated system of triangular lattices.

Taking into account the charge frustration, a possible model of the superstructure of Fe^{2+} and Fe^{3+} in RFe_2O_4 has been proposed[7]. The postulated charge superstructure model is depicted in Fig. 1 for an adjacent iron triangular layer (W-layer). The competing interactions between frustrated charges are settled by this charge arrangement, similar to the stable configuration of Ising spins in triangular lattice[8]. The supercell, which is called a $\sqrt{3} \times \sqrt{3}$ structure, is enlarged by three times in the a–b plane along the (1 1 0) direction. A corresponding superstructure was detected by neutron diffraction. The presence of Bragg spots indexed as $(n/3\ n/3\ m + 1/2)$, where n and m are integers, was found below 330 K. Above 330 K, the spots smeared out to a Bragg line, indexed as $(n/3\ n/3\ l)$, where l takes a continuous value, which indicates the transformation of the three-dimensional (3D) ordering into a two-dimensional one. Below 250 K, the spin correlation develops as a ferrimagnetic ordering[9].

Interestingly, the postulated charge structure allows the presence of a local electrical polarization, since the centres of Fe^{2+} (excess electron) and Fe^{3+} (electron deficiency) do not coincide in the unit cell of the superstructure. This indicates the possibility of ferroelectricity originating from the electron density modulation without a dipole of a cation and anion pair. Therefore, RFe_2O_4 is expected to be a ferroelectric material, reflecting the correlated nature of the electrons. As we show below, a large dielectric dispersion has been found in this material, in which the electron fluctuation has a central role in the ferroelectric domain boundary motion. Also, polarization switching in accordance with the external electric field has been reported. Though these facts suggested the existence of ferroelectricity, they were an insufficient basis on which to predict ferroelectricity by the ordered electrons, because the superstructure of Fe^{2+} and Fe^{3+} was estimated by neutron diffraction which is sensitive to lattice distortion but not to charge.

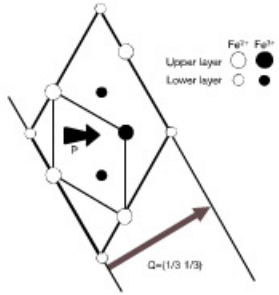

Figure 1 | The charge-ordering model of the double iron layer in RFe_2O_4. The solid lines show the chemical unit cell. The dotted lines show the charge superlattice cell. The Fe ions in upper or lower layers are indicated with a large or a small circle, respectively. Fe^{2+} and Fe^{3+} are represented by open and filled circles, respectively. The polarization P is represented with a short, black arrow. A wave vector Q showing a charge wave is drawn with a long, grey arrow.

[1]Japan Synchrotron Radiation Research Institute, SPring-8, Hyogo 679-5198, Japan. [2]Synchrotron Radiation Research Center, SPring-8, Japan Atomic Energy Research Institute, Hyogo 679-5148, Japan. [3]Japan Atomic Energy Research Institute, Ibaraki 319-1195, Japan. [4]Department of Physics, Tohoku University, Sendai 980-8578, Japan. [5]Department of Physical Science, Osaka Prefecture University, Sakai, Osaka 599-8531, Japan. [6]National Institute of Advanced Industrial Science and Technology, Tsukuba 305-8561, Japan.

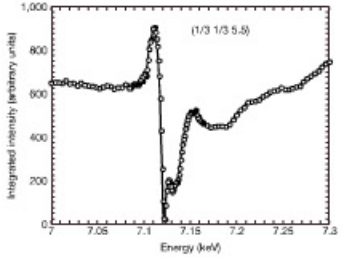

Figure 2 | X-ray energy dependence of the superlattice reflection (1/3, 1/3, 5.5) of a $LuFe_2O_4$ single crystal. Data have been corrected for the absorption effect. The peak and the minimum arise from the in-phase component of the anomalous atomic scattering factor for Fe^{2+} and Fe^{3+}, respectively.

In order to clarify the existence of the superstructure of Fe^{2+} and Fe^{3+}, we performed a resonant X-ray scattering (RXS) experiment, which is the most sensitive technique for detecting the charge superstructure[10–12]. The experiment on single crystal $LuFe_2O_4$ was made with a four-circle diffractometer at beamlines BL02B1 and BL22XU in SPring-8. A crystal sample grown by the floating zone melting method was cut to orient the c axis normal to the sample surface. The intensity of a superlattice spot $(n/3\ n/3\ m + 0.5)$, where n and m are integers, was recorded as a function of the X-ray energy near the K-absorption edge of iron. The sample was cooled in a refrigerator down to 18 K, which is far below the transition temperature.

A typical result of the RXS experiment is displayed in Fig. 2. The absorption effect was corrected in the data. In the spectrum, a maximum and a minimum at around 7.113 keV and 7.120 keV and a background independent of X-ray energy were found. The extrema at 7.113 keV and 7.120 keV arise from the in-phase component of the anomalous atomic scattering factors of Fe^{2+} and Fe^{3+}, respectively. The corresponding K-absorption edges for both ions were confirmed by X-ray absorption near-edge structure measurements for $LuCoFeO_4$ and $LuFeGaO_4$, which are isostructural to RFe_2O_4 but contain only Fe^{3+} and Fe^{2+}, respectively.

This result clearly indicates that the structure factor of this superlattice point is contributed by the positive atomic scattering factor of Fe^{3+} and the negative factor of Fe^{2+}. Therefore, we can conclude that the structure factor at this Bragg point arises from the 'difference' of atomic scattering factors for Fe^{2+} and Fe^{3+}. This is evidence for the formation of the long-range ordering of Fe^{2+} and Fe^{3+} with the $\sqrt{3} \times \sqrt{3}$ structure. This superlattice reflection appears below 330 K, which indicates the development of three-dimensional charge ordering or the occurrence of a Verwey transition. At the same time, spontaneous electric polarization appears below 330 K. This correspondence shows that the charge ordering is an order parameter of the electric polarization.

We demonstrated polarization switching in accordance with the external electric field detected by pyro-electric current observations of single-crystal $LuFe_2O_4$ (ref. 13). In the experiment, the sample was cooled down to 77 K under an electric field of $\pm 10\ kV\ cm^{-1}$ along the c axis, and then the current flow from the sample was recorded upon heating without the electric field. The results showed that the direction of current flow depended on the sign of the cooling electric field below 350 K. We estimated the spontaneous polarization by the integral of the current from the sample. Figure 3 shows the obtained temperature dependence of the electric polarization. A large decrease occurs as the temperature is increased around 250 K, which is the magnetic transition temperature, and at 330 K at which the superstructure of Fe^{2+} and Fe^{3+} appears. This shows that $LuFe_2O_4$ is a polar substance that can be switched by an external electric field, and that the ferroelectricity is developed by the polar arrangement of Fe^{2+} and Fe^{3+}.

The shoulder of the electric polarization at the magnetic transition temperature indicates the coupling of magnetization with electric polarization. In general, magnetic ordering hardly affects electric polarization[14]. But the mechanism described in this Letter, polarization formed by the polar arrangement of Fe^{2+} and Fe^{3+}, may allow such coupling because the coherent arrangement of spins on iron ions give rise to the magnetization. At present we have not investigated this phenomenon completely, but the shoulder suggests that the coherence length of the charge-ordered region or the polarization domain is connected to the development of exchange coupling of iron spins. Though the details are not yet clear, this shoulder demonstrates a potential multiferroic property of ferroelectricity caused by ordered electrons.

Concerning the ferroelectric properties of RFe_2O_4, a characteristic large dispersion had been observed for low frequency alternating current (a.c.) dielectric constants. These are shown in Fig. 4a for $LuFe_2O_4$. The response is the relaxation process expressed by Debye-type dispersion with the amplitude reaching 5,000. Large dielectric dispersion with an amplitude of the order of 10^4 is also observed in the iso-structural family $ErFe_2O_4$ (ref. 15). The dielectric dispersion has a common feature with the order–disorder type of ferroelectric materials, where motion of the ferroelectric domain boundary gives rise to the dispersion. These similarities indicate the presence of the ferroelectric domain and its boundary motion, giving rise to the dispersion.

An analysis of the low-frequency dispersion suggests the origin of this ferroelectricity. At a given temperature, a characteristic response frequency was found at a peak in the frequency variation of the imaginary part of the dielectric constant, ε''. The temperature variation of the characteristic frequency obeys an Arrhenius relation:

$$f = f_0 \exp(-Q/kT) \qquad (1)$$

where f is the characteristic frequency, kT is the thermal energy, f_0 is a prefactor and Q is the activation energy. Observations of the $LuFe_2O_4$ crystal along the c-axis are summarized in Fig. 4b, where $f_0 = 2.8 \times 10^{11}$ Hz and $Q = 0.29$ eV. For comparison, the valence fluctuation frequencies of iron ions obtained by Mössbauer

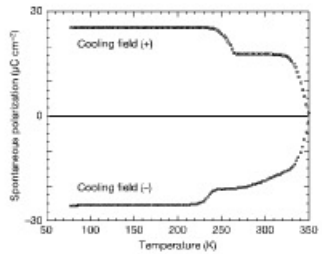

Figure 3 | Temperature variation of the electric polarization of $LuFe_2O_4$. The plot is the integration of a pyro-electric current measurement. The current flow from the sample was recorded on heating after electric field cooling along the c axis. The direction of the electric polarization depends on the direction of electric field, which indicates that $LuFe_2O_4$ possesses macroscopic electric polarization.

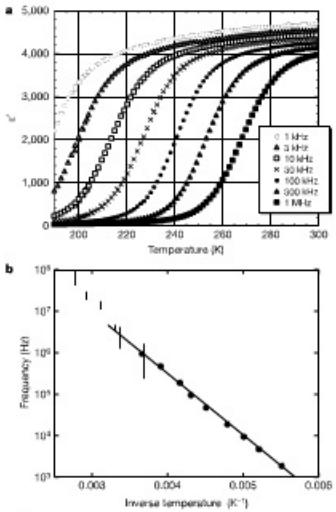

Figure 4 | The a.c. dielectric dispersion in an $LuFe_2O_4$ polycrystalline sample. **a**, The in phase component of the a.c. dielectric constants measured in the frequency range from 1 kHz to 1 MHz. For the observation at 1 kHz, the dielectric constant is more than 4,000 above 220 K. **b**, The temperature variation of the characteristic frequency of the dielectric dispersion. The Arrhenius relation is indicated by a full line. Thick vertical lines represents the iron valence fluctuating frequencies measured with Mössbauer spectroscopy[14]. Extrapolation shows that the electron hopping on the iron ion is the origin of the dispersion.

spectroscopy[16] are marked by thick vertical lines in this figure. The extrapolation of the relation passes through the valence fluctuation frequency, indicating that the electron fluctuation of the iron ions plays a central role in the dielectric response and the motion of the ferroelectric domain boundary. This is consistent with the fact that the polarization arises from the electron ordering. The ferroelectric domain boundary movement proceeds with the exchange of electrons between Fe^{2+} and Fe^{3+} at the domain boundary.

These experimental findings—switching of electric polarization and large dielectric constant—are consistent with a criterion for the existence of ferroelectricity. The order parameter of the electric polarization is the ordering of Fe^{2+} and Fe^{3+} in an arrangement of polar symmetry. The dielectric dispersion shows a typical character of order–disorder type ferroelectric materials where the ferroelectric domain boundary proceeds with electron exchange between Fe^{2+} and Fe^{3+}.

Thus we conclude that $LuFe_2O_4$ is a ferroelectric material, and that this property originates from the polar arrangement of electrons on Fe^{2+}. The electron arrangement arises from charge frustration on a triangular lattice. This arrangement of electrons is realized by the density modulation of *d* electrons, which is different from the premise of electronic ferroelectricity—it is assumed that in a certain kind of transition metal compound with a *d*- and *f*- electron system the balance between electron transfer and electron correlation gives rise to the polar arrangement of electrons. In the case of RFe_2O_4, a particular condition, the charge frustration, leads to the same result: ferroelectricity. This ferroelectricity caused by the electron correlation offers great potential when designing future ferroelectric devices to be coupled or controlled with the degrees of freedom of electrons: charge, spin and orbital. Such properties may lead to a new multiferroic material. Also, the low activation energy of electron motion in this material, which suggests less coupling of polarization switching with the lattice distortion, may enable the development of a fatigue-free solid charge capacitor. These possibilities of new ferroelectric materials will be examined in future studies.

Received 2 May; accepted 11 July 2005.

1. Kittel, C. *Introduction to Solid State Physics* (Wiley, New York, 1995).
2. Cohen, R. E. Origin of ferroelectricity in perovskite oxides. *Nature* **358**, 136–138 (1992).
3. Sághi-Szabó, G., Cohen, R. E. & Krakauer, H. First-principles study of piezoelectricity in $PbTiO_3$. *Phys. Rev. Lett.* **80**, 4321–4324 (1998).
4. Kuroiwa, Y. *et al.* Evidence for Pb–O covalency in tetragonal $PbTiO_3$. *Phys. Rev. Lett.* **87**, 217601 (2001).
5. Portengen, T., Östreich, Th. & Sham, L. J. Theory of electronic ferroelectricity. *Phys. Rev. B* **54**, 17452–17453 (1996).
6. Kimizuka, N., Muromachi, E. & Siratori, K. in *Handbook on the Physics and Chemistry of Rare Earths* Vol. 13 (eds Gschneidner, K. A. Jr & Eyring, L.) 283–384 (Elsevier Science, Amsterdam, 1990).
7. Yamada, Y., Nohdo, S. & Ikeda, N. Incommensurate charge ordering in charge-frustrated $LuFe_2O_4$ system. *J. Phys. Soc. Jpn* **66**, 3733–3736 (1997).
8. Mekata, M. & Adachi, K. Magnetic structure of $CsCoCl_3$. *J. Phys. Soc. Jpn* **44**, 806–812 (1978).
9. Funahashi, S. *et al.* Two-dimensional spin correlation in YFe_2O_4. *J. Phys. Soc. Jpn* **53**, 2688–2696 (1984).
10. Materlik, G., Sparks, C. J. & Fischer, K. *Resonant Anomalous X-Ray Scattering* (North-Holland, Amsterdam, 1994).
11. Sasaki, S. Fe^{2+} and Fe^{3+} ions distinguishable by X-ray anomalous scattering method and its application to magnetite. *Rev. Sci. Instrum.* **66**, 1573–1576 (1995).
12. Murakami, Y. *et al.* Direct observation of charge and orbital ordering in $La_{1-x}Sr_{1+x}MnO_4$. *Phys. Rev. Lett.* **80**, 1932–1935 (1998).
13. Ikeda, N. *et al.* Charge frustration and dielectric dispersion in $LuFe_2O_4$. *J. Phys. Soc. Jpn* **69**, 1526–1532 (2000).
14. Hill, A. N. Why are there so few magnetic ferroelectrics? *J. Phys. Chem. B* **104**, 6694–6709 (2000).
15. Ikeda, N., Kohn, K., Kito, H., Akimitsu, J. & Siratori, K. Dielectric relaxation and hopping of electrons in $ErFe_2O_4$. *J. Phys. Soc. Jpn* **63**, 4556–4564 (1994).
16. Tanaka, M., Siratori, K. & Kimizuka, N. Mössbauer study in RFe_2O_4. *J. Phys. Soc. Jpn* **53**, 760–772 (1984).

Acknowledgements The authors express their gratitude to H. Suematsu and M. Takata for discussions.

 Correspondence and requests for materials should be addressed to N.I. (ikedan@spring8.or.jp).

LETTERS

Catalytic enantioselective reactions driven by photoinduced electron transfer

Andreas Bauer[1], Felix Westkämper[1], Stefan Grimme[2] & Thorsten Bach[1]

Photoinduced electron transfer is an essential step in the conversion of solar energy into chemical energy in photosystems I and II (ref. 1), and is also frequently used by chemists to build complex molecules from simple precursors[2]. During this process, light absorption generates molecules in excited electronic states that are susceptible to accepting or donating electrons. But although the excited states are straightforward to generate, their short lifetimes makes it challenging to control electron transfer and subsequent product formation—particularly if enantiopure products are desired. Control strategies developed so far use hydrogen bonding, to embed photochemical substrates in chiral environments[3] and to render photochemical reactions enantioselective through the use of rigid chiral complexing agents[4]. To go beyond such stoichiometric chiral information transmission, catalytic turnover is required[5]. Here we present a catalytic photoinduced electron transfer reaction that proceeds with considerable turnover and high enantioselectivity. By using an electron accepting chiral organocatalyst that enforces a chiral environment on the substrate through hydrogen bonding, we obtain the product in significant enantiomeric excess (up to 70%) and in yields reaching 64%. This performance suggests that photochemical routes to chiral compounds may find use in general asymmetric synthesis.

In a catalytic photochemical reaction, the catalyst acts as an antenna collecting the light and transferring it to the substrate via sensitization. Sensitization can occur by energy or electron transfer. The most successful enantioselective sensitizers rely on chirality transfer in a conformationally restricted exciplex[6]. The best results reported for a unimolecular reaction are 77% enantiomeric excess (77% e.e.; 20 mol% catalyst) on an analytical scale[7] and for a bimolecular reaction 58% e.e. (15 mol% catalyst) at a product yield of 1% (ref. 8).

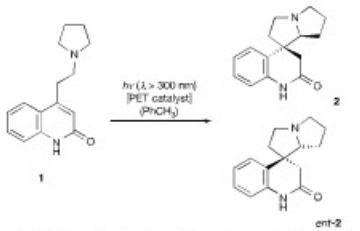

Figure 1 | PET-catalysed cyclization of the prochiral substrate 1 to the chiral pyrrolizidine 2 and its enantiomer ent-2.

The reaction we have devised for studying an enantioselective photoinduced electron transfer (PET) sensitization is depicted in Fig. 1. It is based on previously reported PET catalysed conjugate additions of α-amino alkyl radicals to enones that had been performed non-enantioselectively[9,10]. It proceeds from substrate **1** (see Supplementary Scheme a and Supplementary Information page SI 4) to a chiral spirocyclic pyrrolizidine, which in an achiral environment is obtained as a mixture of **2** and its enantiomer, *ent*-**2**. The simple diastereoselectivity of the reaction is perfect. Only one diastereoisomer is formed, the configuration of which was proved by ^{1}H-NMR nuclear Overhauser effect (NOE) experiments.

In the presence of a catalyst, ultraviolet irradiation induces a PET from the amine to the photoexcited catalyst. Subsequent proton loss from the intermediate cation radical presumably leads to an α-aminoalkyl radical (see also Fig. 3), which adds intramolecularly to carbon atom C-4 of the quinolone. After the radical addition reaction, back electron transfer from the catalyst generates an enolate, which is eventually protonated to yield the products. As mentioned above, similar intramolecular[9] and intermolecular[10] addition reactions to enones are known. A suitable PET catalyst for these reactions was 4,4′-dimethoxybenzophenone (**3**; Fig. 2). By employing ketone **3** as a catalyst (10 mol%), the desired reaction **1** → **2**/*ent*-**2** proceeded in good yield (Table 1, entry 1) but of course without any enantioselectivity. The chiral catalyst **4** that we employed for enantioselective reactions has two key elements. First, it allows for binding of the substrate **1** by two hydrogen bonds at the bridgehead lactam. Second, it contains the catalytic benzophenone unit, which is bound to the 1,5,7-trimethyl-3-azabicyclo[3.3.1]nonan-2-one via a rigid oxazole. It therefore serves not only as a PET catalyst, but also as a stereocontrolling device inducing the desired enantiofacial differentiation in the cyclization step. Indeed, more flexible catalysts were far less successful in the attempted enantioselective reaction. The synthesis of compound **4** and its enantiomer *ent*-**4** was straightforward, based on our previous work (see Supplementary Scheme b and Supplementary Information pages SI 6–8). Experiments were conducted varying the catalyst loading and the substrate concentration. The results are summarized in Table 1.

Even with only 5 mol% catalyst, a reasonable product yield of 61% was obtained (Table 1, entry 2). This gives a calculated turnover number (12.2) that is unprecedented when considering that the product was formed with significant enantiomeric excess (20%). Upon raising the catalyst concentration, the reaction time decreased and the enantioselectivity increased (entries 3, 5, 6). The enantiomeric excess reached 70% for a catalyst loading of 30 mol%, which gave a calculated turnover number of 2.1 (entry 6). Note that these turnover numbers have not been corrected for any uncatalysed processes, even though a racemic background reaction evidently occurs and causes the decrease of e.e. upon decreasing the amount of catalyst (entries 6, 5, 3, 2). In fact, when quinolone **1** was irradiated in

[1]Lehrstuhl für Organische Chemie I, Technische Universität München, Lichtenbergstr. 4, D-85747 Garching, Germany. [2]Universität Münster, Organisch-Chemisches Institut, Corrensstr. 40, D-48149 Münster, Germany.